NIST Special Publication 260
NIST SP 260-249

Certification of Standard Reference Material 2323

Step Height Standard for Areal Surface Topography Measurement

Michael T. Stocker
Thomas B. Renegar
Johannes A. Soons
Ulf Griesmann
Sandra W. Young
Mark R. Stoudt

This publication is available free of charge from:
https://doi.org/10.6028/NIST.SP.260-249

NIST NATIONAL INSTITUTE OF STANDARDS AND TECHNOLOGY
U.S. DEPARTMENT OF COMMERCE

NIST Special Publication 260
NIST SP 260-249

Certification of Standard Reference Material 2323

Step Height Standard for Areal Surface Topography Measurement

Michael T. Stocker
Thomas B. Renegar
Johannes A. Soons
Ulf Griesmann
Sensor Science Division
Physical Measurement Laboratory

Sandra W. Young
Mark R. Stoudt
Materials Science and Engineering Division
Material Measurement Laboratory

This publication is available free of charge from:
https://doi.org/10.6028/NIST.SP.260-249

September 2024

U.S. Department of Commerce
Gina M. Raimondo, Secretary

National Institute of Standards and Technology
Laurie E. Locascio, NIST Director and Under Secretary of Commerce for Standards and Technology

NIST SP 260-249
September 2024

Certain equipment, instruments, software, or materials, commercial or non-commercial, are identified in this paper in order to specify the experimental procedure adequately. Such identification does not imply recommendation or endorsement of any product or service by NIST, nor does it imply that the materials or equipment identified are necessarily the best available for the purpose.

Publication History
Approved by the NIST Editorial Review Board on 2024-09-09

How to Cite this NIST Technical Series Publication
Stocker MT, Renegar TB, Soons JA, Griesmann U, Young SW, Stoudt MR, (2024) Certification of Standard Reference Material 2323 Step Height Standard for Areal Surface Topography Measurement. (National Institute of Standards and Technology, Gaithersburg, MD), NIST Special Publication (SP) NIST SP 260-249.
https://doi.org/10.6028/NIST.SP.260-249

Author ORCID iDs
Michael T. Stocker: 0009-0008-3895-1131
Thomas B. Renegar: 0009-0000-3842-9126
Johannes A. Soons: 0000-0002-9485-1636
Ulf Griesmann: 0000-0001-6882-9729
Sandra W. Young: 0009-0008-5502-8963
Mark R. Stoudt: 0000-0001-8316-6193

Contact Information
stocker@nist.gov

Abstract

We fabricated a set of 64 step height standards, each containing four parallel plateaus offset by three steps of nominally 10 µm, 50 µm, and 100 µm, respectively, and each separated by 18° ramps. The form factor of these standards makes them conducive for introduction into general and forensic-specific areal three-dimensional (3D) surface topography microscopes used in firearm and toolmark evaluations. Each standard is an aluminum cylinder 21.5 mm in diameter and 25 mm tall, similar in diameter of a 12-gauge shotgun shell. The certified step height standards enable customers to calibrate a microscope's z-axis amplification coefficient (vertical scale) and linearity deviation in addition to implementing statistical quality control methods. This publication provides details on the source and preparation of these standards as well as the use of coherence scanning interference microscopy to calibrate the step heights. The uncertainty budget is also described.

Keywords

Areal three-dimensional (3D) microscope, calibration, linearity deviation, metrological characteristic, standard reference material (SRM), step height, surface topography, quality control (QC), vertical amplification coefficient

Table of Contents

List of Tables

List of Figures

Acknowledgments

The authors would like to thank Alan Zheng, Ronald Dixson, and Thomas Germer for review of the document and useful metrology-related discussions. We are grateful to Carlos Beauchamp, Andrew Iams, James Zuback, and Steven Mates for their willingness to share their materials expertise and laboratory resources during the fabrication of the SRM. Special thanks are due to Robert Thompson for his overall guidance of the project and ensuring it remained relevant to the forensic community at large.

1. Introduction

There are two major shifts occurring in forensic firearm and toolmark identification. One is the shift from conventional reflected light microscopy to areal three-dimensional (3D) surface topography microscopy [1-3], which yields the actual 3D topography of the toolmarks instead of an image that is significantly affected by color variations and lighting. The second shift is from subjective similarity evaluations by examiners to objective quantitative similarity metrics [4-12] so that objective decisions regarding common origin can be made with uncertainty statements. Most objective methodologies being considered for forensic firearm identification rely on 3D surface topography measurement of the forensically relevant surfaces on fired cartridge cases and bullets.

Researchers in the United States and abroad, in collaboration with key law enforcement agencies, are working diligently to mature and validate these objective methodologies with the goal of firearm examiners utilizing them in court, supplementing their testimony with similarity scores and associated error rates [13]. In the interim, 3D surface topography measurement has enabled another useful tool for firearm examiners, Virtual Comparison Microscopy (VCM) [14-17]. VCM is a new approach for conducting visual examinations of ballistic evidence. It relies on measuring the actual 3D surface topographies of the samples being evaluated and comparing these 3D sample topographies in a special viewing and comparison software package.

Accurate traceable 3D surface topography data is critical to the successful implementation of future objective methods and VCM in the forensic laboratory. Early adopters of the VCM approach (including the Federal Bureau of Investigation (FBI) and various state and local law enforcement agencies) have already purchased 3D microscopes and are facing increased pressure to validate the accuracy, traceability, and uncertainty of their measurements. Likewise, 3D microscope manufacturers also need valid protocols to validate their instruments.

Documentary standards from the Organization of Scientific Area Committees (OSAC) require forensic service providers (FSP) to adhere to their standards to ensure the 3D instrumentation used in casework is properly calibrated, measurements are traceable, and systems are in statistical control [18]. ISO 25178 is an international standard addressing 3D areal surface texture measurement. [19] Part 600 of this standard describes the metrological characteristics of these types of instruments [19]. A metrological characteristic is any aspect of a measurement instrument that can influence the measurement result. SRM 2323 addresses two metrological characteristics: 1) vertical amplification coefficient (vertical scale) and 2) vertical axis linearity deviation. While commercial products exist for calibrating the metrological characteristics of similar instruments, some systems used in forensic toolmark evaluations are forensic-specific microscopes and only accept firearm and toolmark-related samples.

2. Step Height Design

SRM 2323, shown in Fig. 1, is a 25 mm tall 21.5 mm diameter aluminum cylinder base with four precision pads machined on the top surface. Each pad is at least 3 mm × 3 mm. The pads increase slightly in dimension from top to bottom due to the fabrication process. The 21.5 mm diameter is similar in width to a 12-gauge shotgun shell, enabling introduction into general and forensic toolmark specific microscope systems. The four pads form three vertical steps of 10 µm, 50 µm, and 100 µm. The measurand is the offset between two parallel planes that are a least-squares best fit to the surface measurements of adjacent pads. These vertical steps are calibrated and enable metrological traceability to the International System of Units (SI) for length (meter). The top of the cylindrical base is threaded to receive a nylon protective cap to protect the precision machined surfaces while the SRM is not in use. An 18° transition region (Fig. 2) is incorporated between adjacent pads eliminating surface discontinuities to improve measurability on some 3D surface topography microscopes. The bottom of the unit contains two one-sixteenth inch dowel holes and a metric M5 threaded hole that were used during fabrication. End-users may benefit from using these mounting features when measuring this SRM on their microscope. Mechanical drawings for this SRM unit are provided in Appendices A and B.

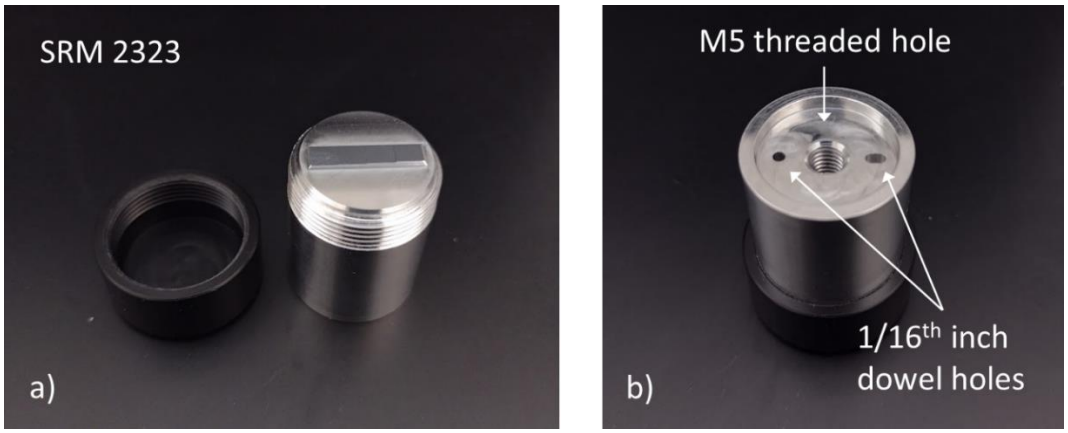

Figure 1. a) SRM 2323 step height standard with nylon protective cap on the left and SRM on the right, b) Bottom view of SRM 2323 showing dowel mounting holes and a threaded M5 hole.

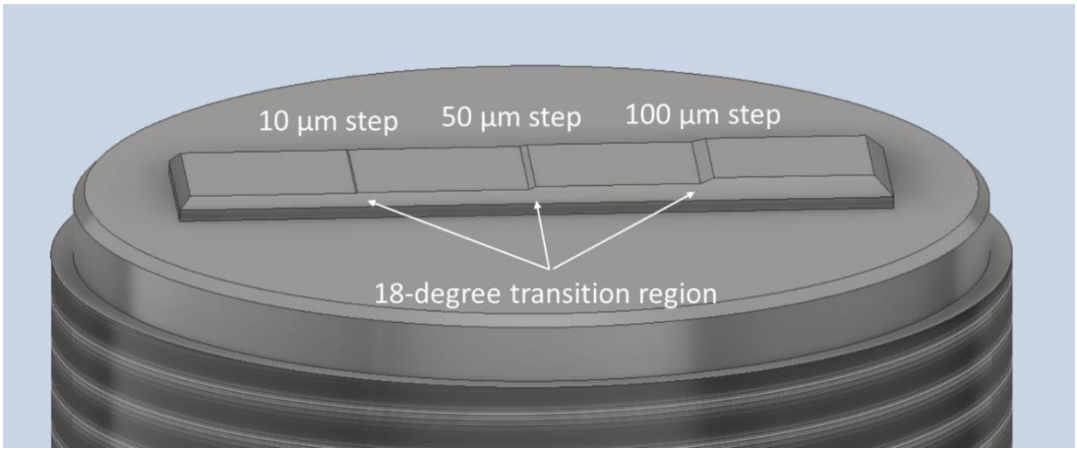

Figure 2. Detail of SRM 2323 showing the three steps and indicating the 18° angular transition region between adjacent pads.

3. Source and Preparation

A total of 64 SRM units were fabricated utilizing both internal machining services at the National Institute of Standards and Technology (NIST) and an external machining contractor. Step height blanks (Fig. 3) and nylon protective caps were produced at NIST using traditional machining operations (e.g., turning, milling). Blanks were made from aluminum alloy 6061-T651. This alloy was chosen primarily for its machinability, especially in the diamond turning process. The external machining contractor utilized single-point diamond turning (SPDT) to further machine the blanks, generating four adjacent pads that comprise the three certified step heights.

SPDT is a specialized turning operation that incorporates a “single-point” diamond as the cutting tool. It is a well-established technique for fabricating precision metal surfaces, leaving an inherently specular surface. Specular surfaces present a challenge for some microscopes utilized in forensic toolmark evaluations. To improve measurability, a chemical etching process was applied to introduce a controlled amount of surface roughness. The etchant used was a 0.5 mol/L NaOH solution. Each sample was immersed in this solution for three minutes, resulting in a root mean square roughness (*Sq*) on the order of 45 nm to 50 nm. The resulting roughness was produced primarily by the preferential attack in the metal grain boundary regions and by the accelerated dissolution of the matrix in the vicinity of surface precipitates, producing a uniform distribution of micrometer-level high-aspect-ratio features on the surface.

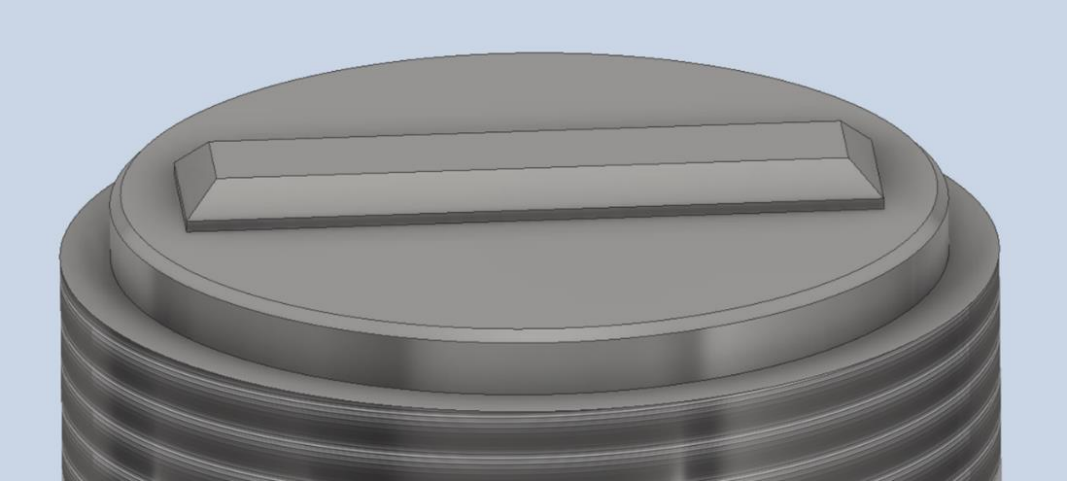

Figure 3. Detail of SRM 2323 blank showing the rectangular island that step planes are machined into.

4. Area-based Surface Topography Certification Method

Calibration of the SRM 2323 step heights was completed using a commercial coherence scanning interferometry (CSI) microscope [20]. A 5.5X magnification objective with a 0.5X tube lens and a 0.55 numerical aperture, yielded a field of view (FOV) of 3.15 mm × 3.15 mm. Single FOV measurements (e.g., no image stitching) were performed for each step height. For each measurement, the sloped area of the step was precisely centered in the FOV of the microscope, and a set of 10 repeat measurements were taken.

The step height was evaluated using the two evaluation areas shown in Fig. 4. Both evaluation areas have the same width w = 1 mm and length L = 2.5 mm. Evaluation area A is located at a distance e = 0.25 mm from the top edge of the step, whereas area B is located at the same distance e from the bottom edge of the step. Fig. 5 illustrates the algorithm that was used to calculate the edge locations in the topography measurements of the steps. The top panel of Fig. 5 shows the cross section of a step on the SRM. The center of the sloped region is found from the magnitude of the first derivative, or gradient, of the step topography measurement by fitting a straight line to the positions of pixels with non-zero first derivative (see center panel of Fig. 5). A slight complication is that the two edges are not identical. Due to the SPDT cutter radius of about 0.1 mm, the inside edge where the sloped region and the bottom pad meet is rounded (Fig. 6). In addition, as a result of the fabrication process, the edges are not straight lines but slightly arcuate, with less than 10 µm deviation from a straight line. This deviation is indicated by δ in Fig. 6.

In practice we found that the difference in the shape of the step edges is of no consequence. The locations of the top and bottom edges of the sloped area are calculated using the magnitude of the second derivative of the topography measurement (bottom panel of Fig. 5). Again, straight lines were fitted to pixel positions with non-zero second derivative. The step algorithm was used to calculate step edge locations and evaluation area placements in a set of 10 repeat measurements of a step. The evaluation area positions had a position standard uncertainty of 0.5 pixels, and the uncertainty in the step height due to the evaluation area placement uncertainty is negligible. Furthermore, we found that even with a larger placement uncertainty for the evaluation areas, the effect on the step height is small. When the placement of area A was varied within ± 3 µm (10 pixels) and the placement of area B within ± 6 µm (20 pixels) the resulting standard uncertainty in the step height evaluation did not exceed 3.5 nm.

A mathematical model of the step is given by

$$Z(x,y) = \propto_x \cdot x + \propto_y \cdot y + \beta + d \cdot \begin{cases} 0, & \text{if } (x,y) \text{ is within area A} \\ -1, & \text{if } (x,y) \text{ is within area B} \end{cases} \quad (1)$$

where Z is the surface height coordinate, $\propto_x$ is the slope in x direction, $\propto_y$ is the slope in y direction, β is an offset, and d is the step height. The parameters of an individual step height, including the step height d, are obtained by fitting the step model in Eq. (1) in a least-squares sense to the evaluation areas A and B of a step height topography measurement.

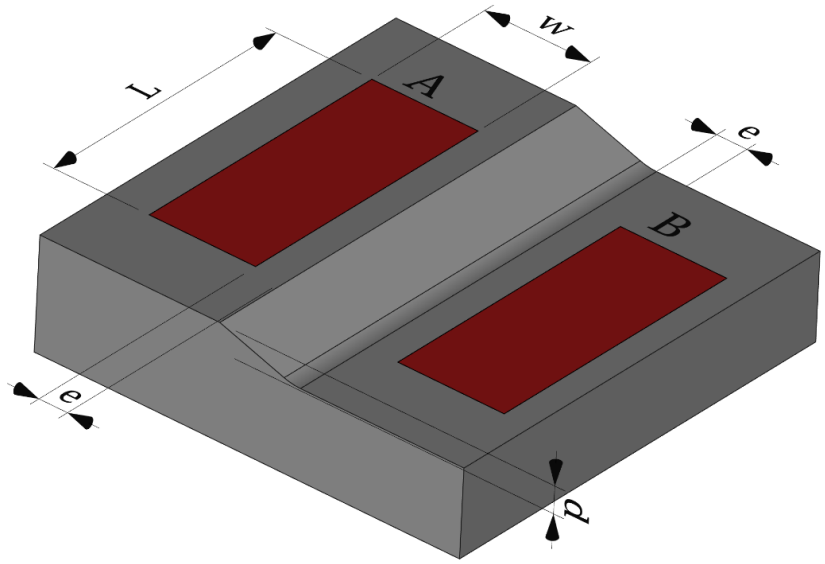

Figure 4. An illustration of one step height on a SRM 2323 step height standard. The two evaluation areas A and B, indicated in red, have a width w = 1 mm, a length L = 2.5 mm, and are located at a distance e = 0.25 mm from their respective edges.

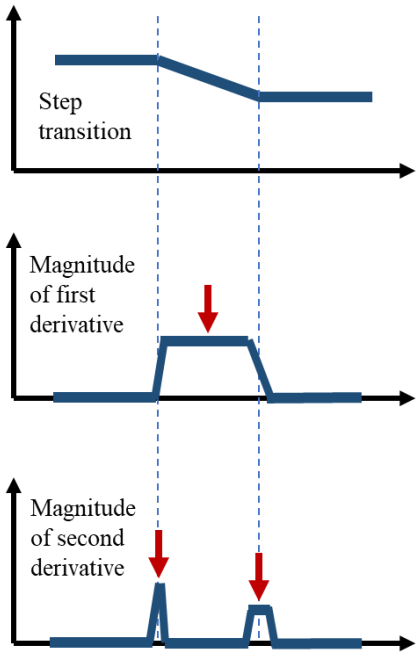

Figure 5. Illustration of the algorithm used to calculate the edge locations in the topography measurements of the steps, incorporating the 1st and 2nd derivatives of the step transition.

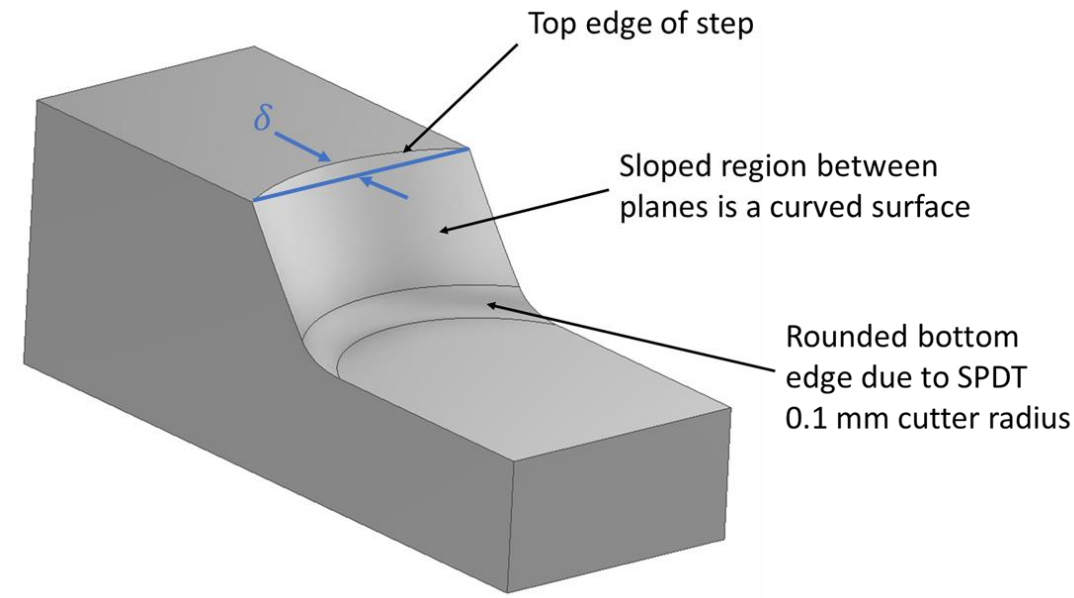

Figure 6. An illustration of rounded top and bottom edges of the steps on SRM 2323. The surface curvature in the sloped region results from how the sample blanks were mounted during machining. The rounding in the bottom edge is due to the radius of the SPDT cutter (Note: The scales are intentionally exaggerated to highlight the geometries.)

4.1. Step Height Measurement Traceability

The metrological traceability provided by SRM 2323 for measurements of the three step heights is established through the calibration process of the z-scan axis of the CSI microscope used to certify the samples [21]. During the z-scan calibration, a narrow-band interference filter with a peak transmission wavelength near 550 nm and a bandwidth of 3 nm is inserted into the light path of the microscope illuminator. The effective wavelength of the narrow-band light is measured in situ with a spectrometer that had its wavelength scale calibrated in the vicinity of 550 nm using the spectral line of mercury at 546.078 nm (at 20 °C, 1013.25 hPa, and 50% relative humidity), emitted by a compact mercury-argon discharge lamp [22-24]. During a z-scan axis calibration, a flat mirror is placed on the test stage, and aligned perpendicular to the z-axis of the interference microscope. An interferogram is then measured over a 145 µm vertical scan using the narrow-band illumination. The actual displacement of the microscope's z-scan axis is derived from the number and spacing of fringes observed during the scan and the known illumination wavelength. This allows a correction factor for the nominal z-axis amplification coefficient to be calculated and establishes traceability of height measurements to the SI meter.

5. Statistical Analysis

For all measurements, the quoted expanded uncertainty U is equal to the combined standard uncertainty u_c times a coverage factor ($k = 2$). The combined standard uncertainty u_c is the positive square root of the sum of the squares of the measurement system standard uncertainty u and the statistical variation of the measurement σ. The statistical variation of the measurement is derived from a gauge repeatability and reproducibility (GR&R) study, where all three steps on one SRM 2323 step height standard were measured over a period of seven days. In this case, the statistical variation of measurement equals the standard deviation of the GR&R measurements. It includes instrument random variation during the measurement process and environmental causes of uncertainty such as vibration and air turbulence. The measurement system standard uncertainty is primarily derived from the uncertainty of the calibration of the interference microscope's z-scan axis. A z-scan axis calibration, described above, results in a correction factor for the nominal vertical amplification coefficient of the z-axis motion system. This calibration procedure has the following contributors to the calibration uncertainty:

a. Traceability of the z-axis calibration to the SI unit meter is achieved through the wavelength of the mercury spectral line at 546.078 nm (calculated from the vacuum wavelength using the refractive index model for air by Birch and Downs [25] at 20 ◦C, an air pressure of 1013.25 hPa, and a relative humidity of 50%). The line has a published wavelength uncertainty of 0.1 pm [22]. The uncertainty of the air wavelength is limited by the variability of air temperature and air pressure in the laboratory.

b. The air temperature within the workspace of the microscope is known to within 0.5 °C resulting in a wavelength uncertainty of the mercury line at 546 nm of 0.3 pm.

c. The atmospheric pressure can deviate from the mean atmospheric pressure within approximately 40 hPa. This atmospheric pressure uncertainty results in an uncertainty of the air refractive index of 1×10^{-5}, and a wavelength uncertainty of the mercury reference line at 546 nm of 5.5 pm.

d. A compact grating spectrometer that is calibrated using the mercury spectral line at 546.078 nm measures the wavelength of the narrow-band illumination source used during z-axis scan calibration. The uncertainty in determining the centroid of the mercury reference line is 0.546 pm. Similarly, the centroid of the narrow-band illumination spectrum is determined with an uncertainty of 1.09 pm.

e. When the wavelength of the calibrated, narrow-band illumination spectrum is determined from the measured interferograms using Fourier transforms, the wavelength uncertainty is found to be 110 pm.

f. During a z-scan axis calibration the numerical aperture of the interference microscope is made as small as practicable to achieve an obliquity factor close to 1. The measured obliquity factor in the preferred z-axis calibration configuration is 1.00042 ± 0.00001.

g. The relative repeatability (standard deviation) of the z-axis amplification factor obtained in multiple z-axis calibrations was found to be 1.75×10^{-4}.

h. The non-linearity in the z-axis scan actuator was evaluated by estimating the local fringe spacing in interferograms measured with narrow-band illumination and a flat reference mirror [26]. The uncertainty of step-height measurements resulting from the z-axis scan non-linearity is given in Table 1. Fig. 7 shows the interpolation of this uncertainty component for all step heights.

i. The measured height of a step height standard may differ from its nominal value due to temperature fluctuations in the laboratory and coefficient of thermal expansion (CTE) of the step height artifact material. For a worst-case CTE of 2.0×10^{-5}/°C and a temperature uncertainty of 0.5 °C, this relative uncertainty is 1.0×10^{-5}.

To reduce random measurement variation due to instrument and environment effects, 10 repeat measurements were made on each step height on each SRM 2323 unit. The mean of these 10 repeatability measurements is the certified value. The statistical variation of measurement, however, came from the GR&R study and not the 10 repeatability measurements. The measurement reproducibility (from the GR&R study), the contribution to the uncertainty due to the non-linearity of the z-axis scan actuator (Fig. 7), and the height dependent uncertainties listed in Table 2 were combined in quadrature to obtain the combined standard uncertainty u_c of the step height calibration [27, 28]. The final expanded uncertainty U_s for the three nominal step height values are shown at the bottom of Table 2. The expanded uncertainty reported by NIST represents only the estimated uncertainty in the NIST calibration of an SRM 2323 step height standard. Additional uncertainties arising in the use of the calibrated specimen, e.g., to transfer a calibrated value to another device, should be evaluated by the customer considering all the influence quantities in the customer's measurement system, including calibration and check standards, instrument, environment, operators, and other factors.

Table 1. The estimated standard uncertainty contribution to a step height measurement resulting from z-axis scan nonlinearity [26].

Step height [µm]	Uncertainty from nonlinearity [nm]	Relative uncertainty [%]
0.01	0.0057	0.0572
0.10	0.0550	0.0550
0.30	0.1457	0.0486
1.00	0.3211	0.0321
3.00	0.4782	0.0159
10.00	0.7923	0.0079
30.00	1.0741	0.0036
80.00	1.3003	0.0016
120.00	8.6594	0.0072
150.00	34.4232	0.0229

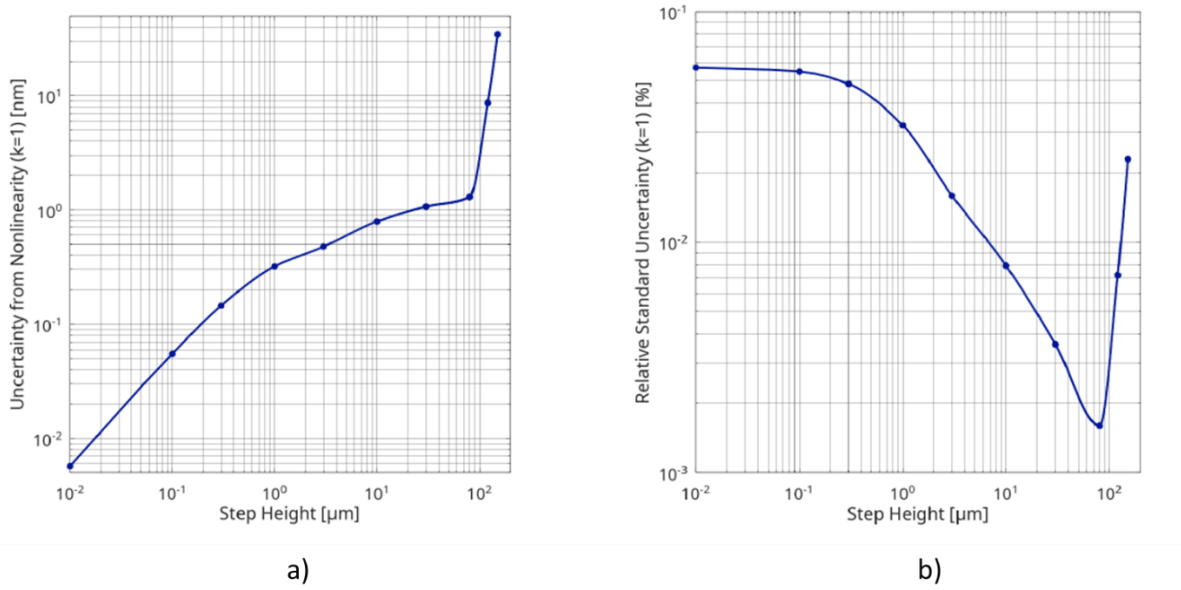

Figure 7. Plot of interpolated standard uncertainty contribution due to z-axis scan non-linearity in Table 1. a) The standard uncertainty contribution as a function of step height, and b) the same as a fraction of the step height [26].

Table 2. The top rows list contributors to the measurement uncertainty that are independent of the step height standard under test. The combined and expanded uncertainties (in the last two rows) are calculated using the procedures described in [27, 28]. The value h in the right column represents the nominal step height value in nanometers. The final expanded uncertainty $U_s = k \times u_c$ where $k = 2$ are shown in the bottom row.

Description	Uncertainty	Effect on step height h
Uncertainty in the air wavelength value of the mercury spectral line at 546.078 nm due to variability of air temperature and air pressure	5.5 pm	$h \times (1.01 \times 10^{-5})$
Uncertainty in the centroid estimation of the mercury spectral line at 546.078	0.546 pm	$h \times (1.01 \times 10^{-6})$
Uncertainty in the centroid estimation of the narrow-band illumination used for z-axis amplification factor calibration	1.09 pm	$h \times (2.01 \times 10^{-6})$
Z-axis amplification factor calibration repeatability	1.75×10^{-4}	$h \times (1.75 \times 10^{-4})$
Uncertainty of the measured obliquity factor	1.0×10^{-5}	$h \times (1.0 \times 10^{-5})$
Uncertainty of the narrow-band illumination centroid wavelength as determined from interferograms	110 pm	$h \times (2.01 \times 10^{-4})$

measured with the interference microscope		
Uncertainty in the step height measurement resulting from the z-axis scan non-linearity [26]	0.79 nm (for 10 µm step) 1.19 nm (for 50 µm step) 3.69 nm (for 100 µm step)	$h \times (7.9 \times 10^{-5})$ $h \times (2.38 \times 10^{-5})$ $h \times (3.69 \times 10^{-5})$
Uncertainty of step height due to the material's coefficient of thermal expansion	1.0×10^{-5}	$h \times (1.0 \times 10^{-5})$
The statistical variation of measurement based on GR&R results per each nominal step height value		3.1 nm (for 10 µm step) 12.9 nm (for 50 µm step) 15.3 nm (for 100 µm step)
	Combined Standard Uncertainty (u_c):	4.2 nm (for 10 µm step) 19 nm (for 50 µm step) 31 nm (for 100 µm step)

Expanded Uncertainty U_s ($k = 2$)
(where s equals the nominal step height in micrometers)

$U_{10} = 8.4$ nm	$U_{50} = 38$ nm	$U_{100} = 62$ nm

6. References

[1] Senin, Nicola, et al. "Three-dimensional surface topography acquisition and analysis for firearm identification." *Journal of forensic sciences* 51.2 (2006): 282-295.

[2] Weller, Todd J., et al. "Confocal microscopy analysis of breech face marks on fired cartridge cases from 10 consecutively manufactured pistol slides." *Journal of forensic sciences* 57.4 (2012): 912-917.

[3] Vorburger, T. V., Song, J., and Petraco, N. "Topography measurements and applications in ballistics and tool mark identifications." *Surface topography: metrology and properties* 4.1 (2015): 013002.

[4] Chu, Wei, et al. "Automatic identification of bullet signatures based on consecutive matching striae (CMS) criteria." *Forensic science international* 231.1-3 (2013): 137-141.

[5] Chumbley, L. S., et al. "Validation of tool mark comparisons obtained using a quantitative, comparative, statistical algorithm." *Journal of Forensic Sciences* 55.4 (2010): 953-961.

[6] Ma, Lijie, et al. "NIST bullet signature measurement system for RM (Reference Material) 8240 standard bullets." *Journal of forensic sciences* 49.4 (2004): 649-659.

[7] Petraco, N. D., et al., "Application of Machine Learning to Toolmarks: Statistically Based Methods for Impression Pattern Comparisons," NIJ Report 239048, National Institute of Justice, Washington DC, July 2012, <https://www.ncjrs.gov/pdffiles1/nij/ grants/239048.pdf>.

[8] Song, J. "Proposed NIST ballistics identification system (NBIS) based on 3D topography measurements on correlation cells." *AFTE Journal* 45.2 (2013): 184-194.

[9] Song, J., et al. "SRM 2460/2461 standard bullets and casings project." *Journal of research of the National Institute of Standards and Technology* 109.6 (2004): 533.

[10] Tai, Xiao Hui, and Eddy, W. F. "A fully automatic method for comparing cartridge case images." *Journal of forensic sciences* 63.2 (2018): 440-448.

[11] Roberge, D., Beauchamp, A., and Lévesque, S. "Objective identification of bullets based on 3D pattern matching and line counting scores." *International Journal of Pattern Recognition and Artificial Intelligence* 33.11 (2019): 1940021.

[12] Riva, F., and Champod, C. "Automatic comparison and evaluation of impressions left by a firearm on fired cartridge cases." *Journal of forensic sciences* 59.3 (2014): 637-647.

[13] Song, J., et al. "Estimating error rates for firearm evidence identifications in forensic science." *Forensic science international* 284 (2018): 15-32.

[14] Weller, Todd, et al. "Introduction and initial evaluation of a novel three-dimensional imaging and analysis system for firearm forensics." *AFTE J* 47.4 (2015): 198-208.

[15] Lilien, R. "Applied research and development of a three-dimensional topography system for firearm identification using gelSight." *USA Patent No* 248639 (2015).

[16] Chapnick, C., et al. "Results of the 3D virtual comparison microscopy error rate (VCMER) study for firearm forensics." *Journal of forensic sciences* 66.2 (2021): 557-570.

[17] Knowles, L., Hockey, D., and Marshall, J. "The validation of 3D virtual comparison microscopy (VCM) in the comparison of expended cartridge cases." *Journal of Forensic Sciences* 67.2 (2022): 516-523.

[18] ANSI/ASB Standard 061, 1st Ed., Firearms and Toolmarks 3D Measurement Systems and Measurement Quality Control, 2021.

[19] ISO 25178-600:2019, *Geometrical product specifications (GPS)– Surface texture: Areal – Part 600: Metrological characteristics for areal topography measuring methods*, International Organization for Standardization (ISO), Geneva (2019)

[20] De Groot, P. "Principles of interference microscopy for the measurement of surface topography." *Advances in Optics and Photonics* 7.1 (2015): 1-65.

[21] de Groot, P., and Beverage, Jake. "Calibration of the amplification coefficient in interference microscopy by means of a wavelength standard." *Modeling Aspects in Optical Metrology V*. Vol. 9526. SPIE, 2015.

[22] Sansonetti, C. J., Salit, M. L., and Reader, J., *Wavelengths of spectral lines in mercury pencil lamps*, Applied Optics 35, 74-77 (1996)

[23] Kaufman, V., *Wavelengths, energy levels, and pressure shifts in mercury-198*, Journal of the Optical Society of America 52, 866-870 (1962).

[24] Reader, J., *Metrological implications of recent interferometricwavelength measurements for singly ionized silicon in the vacuum ultraviolet (*152 nm *and* 180 nm*)*, Metrologia 39, 391-394 (2002)

[25] Birch, K. P., and Downs, M. J., *Correction to the updated Edl´en equation for the refractive index of air*, Metrologia 31, 315-316 (1994)

[26] Germer, T. A., Renegar, T. B., Griesmann, U., and Soons, J. A., *Linearizing the vertical scale of an interferometric microscope and its effect on step-height measurement*, Surf. Topogr.: Metrol. Prop. 12, 025012 (2024)

[27] Taylor, B. N., and Kuyatt, C. E., *Guidelines for Evaluating and Expressing the Uncertainty of NIST Measurement Results*, NIST Technical Note 1297, National Institute of Standards and Technology, Gaithersburg, Maryland (1994)

[28] Possolo, A. *Simple Guide for Evaluating and Expressing the Uncertainty of NIST Measurement Results*, NIST Technical Note 1900, National Institute of Standards and Technology, Gaithersburg, Maryland (2015)

7. Appendix A. Mechanical Drawings for SRM 2323 Blanks

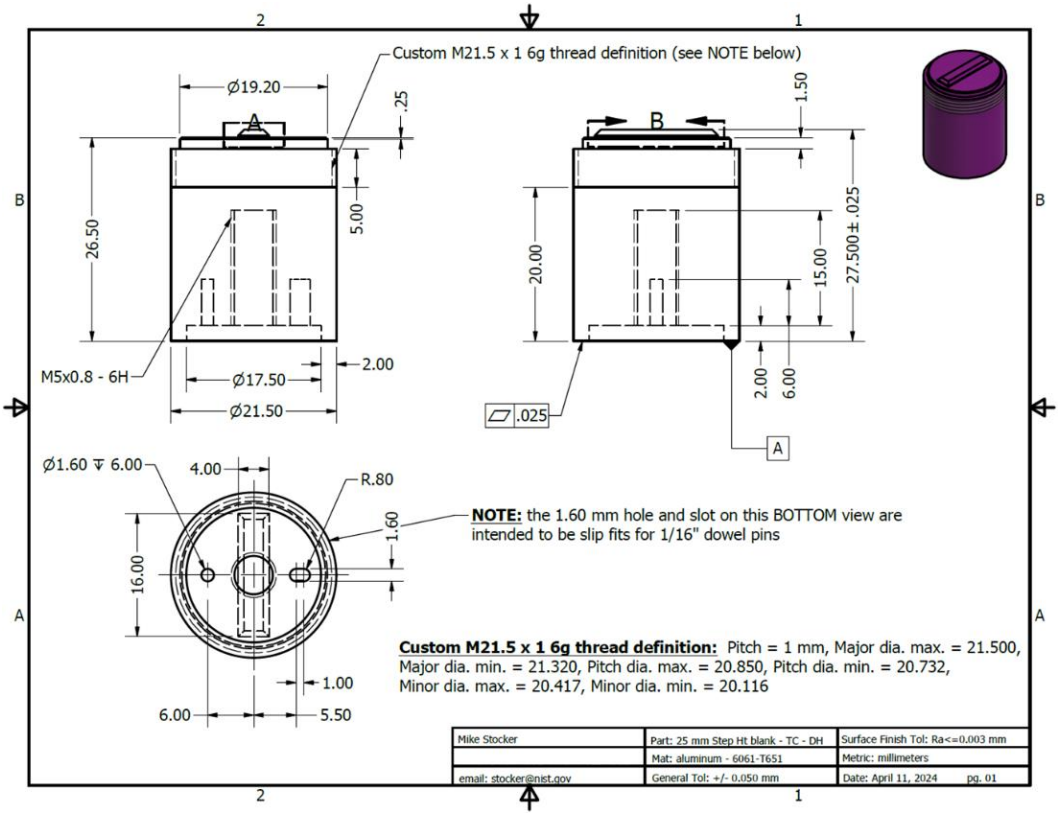

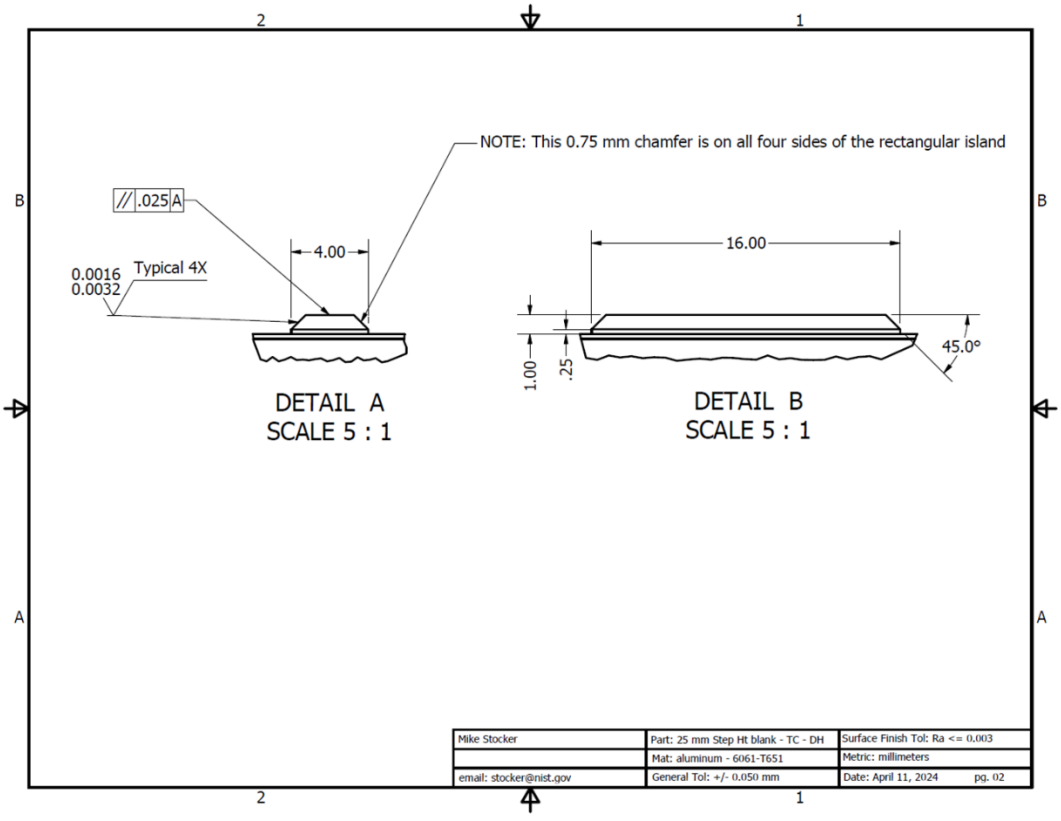

8. Appendix B. Mechanical Drawings for SRM 2323 Final Step Height Dimensions